Quantum teleportation and entanglement swapping with linear optics logic gates

2009 New J. Phys. 11 033008

(http://iopscience.iop.org/1367-2630/11/3/033008)

New Journal of Physics
The open-access journal for physics

Quantum teleportation and entanglement swapping with linear optics logic gates

Christian Schmid[1,2,5], Nikolai Kiesel[1,2], Ulrich K Weber[3], Rupert Ursin[4], Anton Zeilinger[4] and Harald Weinfurter[1,2]

[1] Department für Physik, Ludwig-Maximilians-Universität, D-80797 München, Germany
[2] Max-Planck-Institut für Quantenoptik, D-85748 Garching, Germany
[3] Materials Department, University of Oxford, Oxford OX1 3PH, UK
[4] Fakultät für Physik, Universität Wien, A-1090 Wien, Austria
E-mail: christian.schmid@mpq.mpg.de

New Journal of Physics **11** (2009) 033008 (10pp)
Received 20 November 2008
Published 4 March 2009
Online at http://www.njp.org/
doi:10.1088/0031-8949/11/3/033008

Abstract. We report on the usage of a linear optics phase gate for distinguishing all four Bell states simultaneously in a quantum teleportation and entanglement swapping protocol. This is demonstrated by full-state tomography of the one- and two-qubit output states of the two protocols, yielding average state fidelities of about 0.83 and 0.77, respectively. In addition, the performance of the teleportation channel is characterized by the quantum process tomography. The non-classical properties of the entanglement swapping output states are further confirmed by the violation of a CHSH-type Bell inequality of 2.14 on average.

Contents

[5] Author to whom any correspondence should be addressed.

1. Introduction

Quantum teleportation [1] and entanglement swapping [2] are fundamental elements of quantum communication protocols and thus play an important role in a number of applications. Both processes rely on the projection of two qubits onto maximally entangled Bell states. As every qubit can be analysed only separately, this detection requires the four Bell states to be mapped one-to-one onto four distinguishable, separable states. Such a disentangling operation can be realized by elementary two-qubit quantum gates, e.g. a controlled-NOT (CNOT) or controlled phase (CPHASE) gate. Teleportation has been demonstrated already with a number of different systems, where the gate operations can be achieved (e.g. [3]–[6]). However, while photons doubtlessly are the most proper quantum system for communication tasks, the implementation of two-photon quantum gates is not straightforward as there is no photon–photon interaction with reasonable coupling strength[6]. Beginning with the initial experiments [9, 10], two-photon interference [11, 12] was employed to identify up to two of the four Bell states and, recently, a probabilistic identification of three Bell states using positive operator-valued measure (POVM)-operators was demonstrated [13]. As introduced by Knill, Laflamme and Milburn (KLM) [14], all optical two-qubit quantum logic can be achieved nearly deterministically using linear optics plus conditioned detection and ancillary qubits. The latter can be omitted when probabilistic gate operation is sufficient [15, 16]. Several experiments have already proved the feasibility of these approaches (see [17]–[19] or [20], respectively). Recently, a significant improvement with respect to reliability and stability of a linear optics logic gate was reported [21]–[25] which allows such gates to be employed in multi-photon quantum communication protocols. Here, we report on the implementation of quantum teleportation and entanglement swapping including probabilistic, complete Bell state analysis (BSA) accomplished by the use of a linear optics CPHASE gate.

2. Experiment

2.1. The Bell-state measurement

Let us start by briefly sketching the functionality of the gate [22]. The operation is defined by

$$\text{CPHASE} = \begin{cases} |HH\rangle & \rightarrow & |HH\rangle, \\ |HV\rangle & \rightarrow & |HV\rangle, \\ |VH\rangle & \rightarrow & |VH\rangle, \\ |VV\rangle & \rightarrow & -|VV\rangle, \end{cases} \tag{1}$$

where the logical 0 and 1 are represented by the linear horizontal (H) and vertical (V) polarization states of a photon, respectively. To obtain the π-phaseshift for the term $|VV\rangle$ only, the gate-input photons are overlapped on a beam splitter with polarization-dependent splitting ratio (PDBS), where the transmission for horizontal polarization $T_{\mathrm{H}} = 1$, and for vertical polarization $T_{\mathrm{V}} = 1/3$. As horizontal polarization is not affected, no interference can occur for $|HH\rangle$ and the state does not change. The same holds for $|HV\rangle$ and $|VH\rangle$ where the photons are distinguishable by polarization and therefore do not interfere. Only if two vertically

[6] The quantum teleportation of a photon polarization state with complete Bell state analysis was once demonstrated using nonlinear effects, though with vanishingly small probability [7]. Deterministic schemes relying on entanglement in additional degrees of freedom are not suited for teleportation [8].

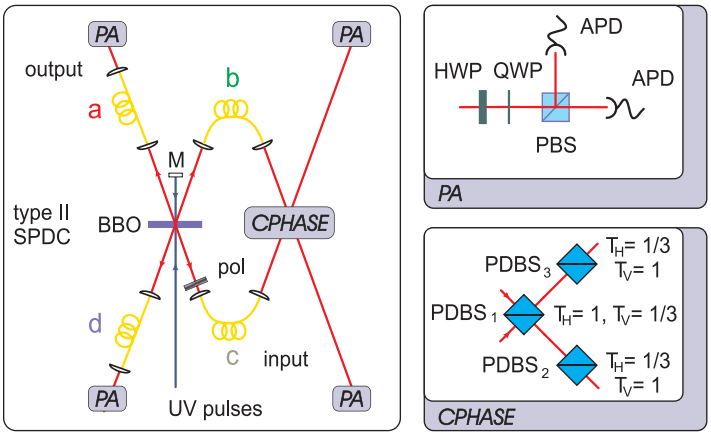

Figure 1. Experimental setup for the quantum teleportation and the entanglement swapping experiment, respectively. The three- and four photon states are provided by two Einstein–Podolsky–Rosen (EPR)-pairs originating from type II SPDC processes. UV pulses are used to pump a BBO crystal twice. If a photon pair is created in each of the two passages, teleportation or entanglement swapping can be performed. After passing the crystal, the beam is reflected back by a UV-mirror (M). HWP and QWP in conjunction with PBSs are used for the PA. The complete BSA is done by a CPHASE gate consisting of three PDBS ($PDBS_1$–$PDBS_3$). The photons are spectrally selected with interference filters.

polarized photons pass the gate does two-photon interference occur. For this case, we obtain a π-phaseshift if the ratio of the amplitudes for both photons being reflected is greater than the one for both being transmitted. In order to obtain equal amplitudes for all four output states a transmission $T_V = 1/3$ is required, together with two beam splitters with reversed splitting ratio ($T_H = 1/3$, $T_V = 1$) placed after each output of the PDBS (see figure 1). The gate operation succeeds if one photon is detected in each of the two outputs of the gate, which occurs in 1/9 of all cases.

The CPHASE gate can be used to perform a complete Bell-state projection measurement by mapping four Bell states onto four orthogonal product states [21]. Considering as input, for example, the maximally entangled Bell state $|\tilde{\phi}^+\rangle = 1/\sqrt{2}(|H+\rangle + |V-\rangle)$, where $+(-)$ denotes $+45°(-45°)$ linear polarization, the gate will do the following operation:

$$\begin{aligned} |\tilde{\phi}^+\rangle &= \tfrac{1}{2}\,(|HH\rangle + |HV\rangle + |VH\rangle - |VV\rangle), \\ &\overset{\text{CPHASE}}{\rightleftharpoons} \tfrac{1}{2}\,(|HH\rangle + |HV\rangle + |VH\rangle + |VV\rangle), \\ &= \tfrac{1}{2}\,(|H\rangle + |V\rangle) \otimes (|H\rangle + |V\rangle) = |{+}{+}\rangle. \end{aligned} \tag{2}$$

This means, the gate transforms between the product state $|{+}{+}\rangle$ and the maximally entangled Bell state $|\tilde{\phi}^+\rangle$ (analogously we obtain for $|\tilde{\psi}^+\rangle \rightleftharpoons |{+}{-}\rangle$, $|\tilde{\phi}^-\rangle \rightleftharpoons |{-}{+}\rangle$ and $|\tilde{\psi}^-\rangle \rightleftharpoons |{-}{-}\rangle$). Consequently, by detecting one of these four product states *behind* the phase gate, we know that the photons have been in the corresponding Bell state *before* the phase gate.

For quantum teleportation and entanglement swapping it is, in principle, not necessary to project onto all four Bell states to perform these protocols. The first realizations indeed used the projection onto a single Bell-state only, neglecting the other cases. This results in a

success probability of 1/4 [9, 10]. The best success probability achieved is 1/2 and is known to be the theoretical limit when using linear optics without ancillary qubits [11, 12, 26, 27]. Even though we do not neglect any Bell state in our scheme, our success probability is limited by the efficiency of the gate operation, which is 1/9, and therefore lower than in the other schemes. However, the beauty of the application of the CPHASE gate is the possibility to detect all four Bell states in a setup just as simple as the (single-state) Bell-state projection of the initial demonstration of quantum teleportation [9].

Moreover, for quantum teleportation and entanglement swapping one might even mimic the detection of all four Bell states with a setup that detects only a restricted number, by randomly switching between the detected set of states. We would like to emphasize, however, that this approach relies only on a statistical mixture of all four Bell states. In contrast, in a CPHASE gate scheme, a coherent superposition of all Bell states is obtained. This is a fundamental difference and might be crucial for other tasks that rely on the detection of Bell states. Such a situation is present, e.g. in the quantum games scheme, where the referee relies on a quantum gate to analyse entangled states [28]. As discussed before, the referee will, due to the limited success probability of BSA, have to discard several games. But by detecting coherently all four states he does not give the players any chance to cheat, as might be possible for other BSA implementations. Another scheme was recently reported in which the detection of four Bell states by the CPHASE gate could be used for the direct experimental observation of mixed state entanglement [29].

2.2. Photon state preparation and detection

In the experiment, the input states for teleportation and entanglement swapping are generated with spontaneous parametric down conversion. A 2 mm thick β-barium borate (BBO) crystal is pumped by UV pulses with a central wavelength of 390 nm and an average power of 700 mW from a frequency-doubled mode-locked Ti:sapphire laser (pulse length 130 fs). After passing the crystal the beam is reflected back by a UV-mirror at a distance of about 3 cm to enable spontaneous parametric down conversion (SPDC) also into a second pair of beams. We use degenerate, non-collinear type-II phase matching to obtain pairs of orthogonally polarized photons at a wavelength of $\lambda \simeq 780$ nm in the forward and backward directions of the BBO crystal, respectively. The photons propagating along the characteristic intersection lines of the emission cones are coupled into single-mode fibres defining the four spatial modes a, b, c and d. The spectral selection is done with narrow bandwidth interference filters F ($\Delta\lambda = 2$ nm in the CPHASE gate and $\Delta\lambda = 3$ nm in modes a and d) before detection. For initial alignment of the spatial overlap at the partially polarizing beam splitter (PBS) in the CPHASE gate we use the two photons of one pair for higher count rates, whereas the temporal overlap can be aligned via Hong–Ou–Mandel interference of two independently created, heralded single photons in the forward and backward directions (see figure 1). The polarization states of the photonic qubits are analysed by half- and quarter wave plates (HWP and QWP) in combination with a PBS cube and detected by avalanche photon diodes (APD). The setup is stable over several days with typical detection rates of 180 fourfold coincidence counts per hour. The coincidence count rates have to be corrected for different detector efficiencies in the polarization analysis (PA) of modes a, b, c and d, which are determined relative to each other. The errors on all quantities are deduced according to Poissonian counting statistics of the raw detection events and the detection efficiencies.

2.3. Teleportation

The goal of quantum teleportation is to transfer the most general polarization state $|\chi\rangle_c = (\alpha|H\rangle_c + \beta|V\rangle_c)$ with arbitrary amplitudes α and β of the photon in mode c onto the photon in mode a. In order to do so, we need, firstly, a maximally entangled Bell state in modes a and b, and, secondly, a complete Bell-state projection measurement between the photons in modes b and c. We obtain the Bell state by proper alignment of the photon pair originating from the forward downconversion. The photon that will carry the state $|\chi\rangle_c$ is provided by the backward emission of the down conversion, which is operated as a heralded single-photon source with the photon in mode d initializing the trigger. The polarization state $|\chi\rangle_c$ can be prepared by a polarizer in front of the fibre coupler in mode c and proper alignment of the fibre's polarization controller.

To demonstrate teleportation, we have prepared the states $|H\rangle$, $|V\rangle$, $|+\rangle$, $|R\rangle = 1/\sqrt{2}\,(|H\rangle + \mathrm{i}|V\rangle)$ as input states and carried out a single-qubit tomography [30] in the output mode a. From this we obtain the density matrix ρ_{exp} of the experimentally teleported states and can calculate the fidelities to the input states, $\mathcal{F}_H = 0.93 \pm 0.02$, $\mathcal{F}_V = 0.75 \pm 0.05$, $\mathcal{F}_+ = 0.79 \pm 0.02$ and $\mathcal{F}_R = 0.84 \pm 0.03$, with

$$\mathcal{F}_k = {}_c\langle\chi_k|\mathcal{U}_i\rho_{\mathrm{exp}}\mathcal{U}_i^{\dagger}|\chi_k\rangle_c, \tag{3}$$

where $k = H, V, +$ and R.

Depending on the outcome of the Bell projection measurement one has to apply one out of four unitary operations (represented by the identity or one of the three Pauli matrices, respectively, $\mathcal{U}_i = \mathbb{1}, \sigma_x, \sigma_z$ or $\mathrm{i}\sigma_y$) in order to recover the original state in the teleported mode. Therefore, the fidelities are calculated after application of the unitary operation on the data and averaging over the four different results of the BSA.

As can be seen, the quality of the output states differs for the various input states. This can be understood by considering the influence of imperfect gate operation. For the experimental gate the main reason for deviation from ideal performance is caused by lack of interference at PDBS_1. From the considerations in section 2.1 it can be easily seen that for perfectly distinguishable photons the probability of obtaining a coincidence detection is enhanced by a factor of five for the input state $|VV\rangle$. This is because if the photons do not interfere, the probabilities rather than the amplitudes for both being reflected or both being transmitted add up to $(1/3)^2 + (-2/3)^2 = 5/9$.

Taking that into account, it is obvious that the teleportation works best for the state $|H\rangle$, as in this instance no interference is required. Consequently, from this point of view, the output state for the input $|V\rangle$ is expected to be the worst. The states $|+\rangle$ and $|R\rangle$ should be teleported approximately at the same quality on average. However, for the state $|+\rangle$ the fidelity of the output state depends on the result of the measurement in the CPHASE gate. The measured fidelities exhibit roughly the expected behavior: the loss in quality for $|H\rangle$ is not caused by lack of interference but determined by impurity of the input states. For $|R\rangle$, $|+\rangle$ and $|V\rangle$ both effects are relevant. However, $|V\rangle$ is maximally impaired by the imperfect interference and exhibits indeed the lowest fidelity. Still, despite all imperfections it is important to note that the average fidelities are all well above the optimal classical limit of $2/3$.

The four chosen input states represent a tomographic set out of which we can evaluate a teleportation process tomography [31]. From this tomography one obtains the matrix $\mathcal{M}_{\mathrm{exp}}$

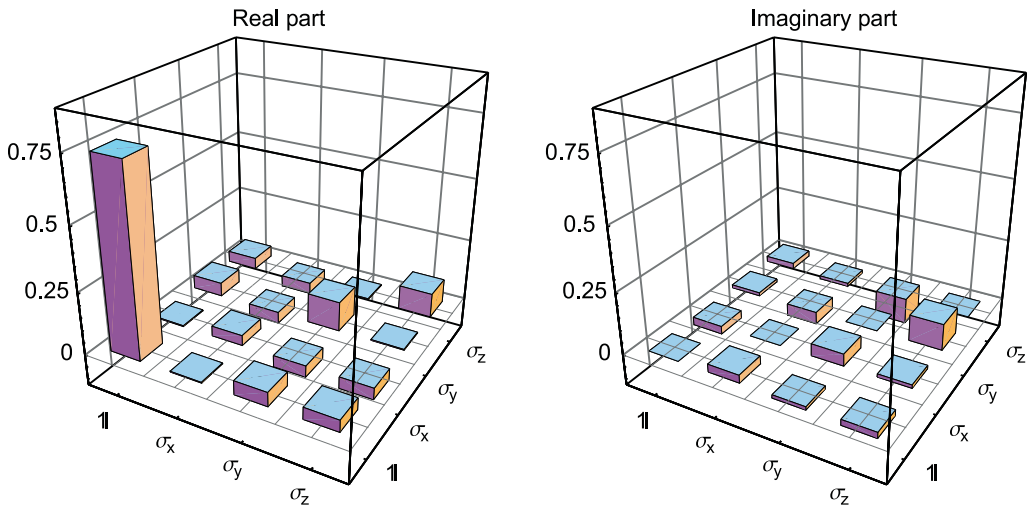

Figure 2. Experimentally reconstructed teleportation process tomography matrix $\mathcal{M}_{\text{exp}}$. As the ideal teleportation process equals the $\mathbb{1}$-operation, the height of the $(\mathbb{1}, \mathbb{1})$-entry of $\mathcal{M}_{\text{exp}}$ serves directly as a measure for the fidelity of the experimentally achieved process. The smallness of the imaginary parts, which are all below 0.1, also confirms the quality of our teleportation procedure.

representing the performance of the teleportation process[7] (see figure 2). In this representation an ideal teleportation ($\mathcal{M}_{\text{theo}}$) corresponds to the identity operation. Thus the height of the $(\mathbb{1}, \mathbb{1})$-entry of $\mathcal{M}_{\text{exp}}$ directly gives the so-called process fidelity [33]:

$$F_{\text{p}} = \text{Tr}[\mathcal{M}_{\text{theo}}\mathcal{M}_{\text{exp}}], \tag{4}$$

which is the overlap between the experimentally obtained and the theoretically expected matrix, and which is the measure for the quality of the implemented teleportation process. In our experiment we reached $F_{\text{p}} = 0.75$. The limiting factor for the process fidelity is the fidelity of the state which is teleported worst. Following the previous discussions this is the state $|V\rangle$ for which the output state fidelity reaches an average value comparable to F_{p}.

2.4. Entanglement swapping

The inherent quantum features of the teleportation process are best seen by performing entanglement swapping. In this quantum communication method two photons, which have never interacted in the past, become entangled by teleporting the state of one photon of an entangled pair onto one photon of another entangled pair. In the experiment described before, the teleportation of a polarized photon does not always succeed, e.g. due to experimental restrictions like limited detection efficiencies. Hence, it could be argued that the observed teleportation fidelities are a result of statistical averaging over many measurements. Such arguments can be directly refuted for entanglement swapping. Here, the teleported photon is part of an entangled pair, in the sense that it is not polarized. Therefore, the outcome of a measurement on this photon

[7] Note that we do not use the process tomography to characterize the two-qubit logic gate, as was demonstrated in [32]. Instead, we use it to describe the teleportation channel as a quantum process mapping one-qubit input states onto one-qubit output states.

Table 1. Experimental results obtained in the entanglement swapping experiment.

Bell-state observed	Fidelity ($\mathcal{F}_{\text{exp}}$)	Negativity ($\mathcal{N}$)
$\lvert\tilde{\phi}^+\rangle_{cb}$	0.777 ± 0.031	0.660 ± 0.051
$\lvert\tilde{\psi}^+\rangle_{cb}$	0.776 ± 0.029	0.666 ± 0.048
$\lvert\tilde{\phi}^-\rangle_{cb}$	0.736 ± 0.031	0.582 ± 0.055
$\lvert\tilde{\psi}^-\rangle_{cb}$	0.803 ± 0.027	0.720 ± 0.042

only is completely random. If the observed teleportation results for individual one-photon output states were attributed to statistical averaging, the analogous experimental procedure would thus unavoidably lead to a random result for the correlation measurements on two-photon output states. In the following, however, it will be proven that indeed quantum correlations can be observed. This confirms the entanglement contained in the swapped photon pair and proves that teleportation succeeds for every single instance.

To perform entanglement swapping we start with two entangled photon pairs, each in the state $|\phi^+\rangle = 1/\sqrt{2}(|HH\rangle + |VV\rangle)$ emitted by our down conversion source in the forward and in the backward directions, respectively. As before, we accomplish the Bell projection measurement between modes b and c by the use of the CPHASE gate. Consequently, by projecting photons from these two modes onto a Bell state, the photons from modes a and d will be left in a maximally entangled state. Which Bell state they form again depends on the result of the Bell-state measurement in modes b and c:

$$|\Psi\rangle_{abcd} = |\phi^+\rangle_{ab}|\phi^+\rangle_{cd} = \tfrac{1}{2}\Big(|\tilde{\phi}^+\rangle_{ad}|\tilde{\phi}^+\rangle_{bc} + |\tilde{\psi}^+\rangle_{ad}|\tilde{\psi}^+\rangle_{bc} + |\tilde{\phi}^-\rangle_{ad}|\tilde{\phi}^-\rangle_{bc} + |\tilde{\psi}^-\rangle_{ad}|\tilde{\psi}^-\rangle_{bc}\Big). \quad (5)$$

In order to determine how close the experimentally obtained states are to the expected ones and whether they are indeed entangled we performed a two-qubit tomography for photons detected in modes a and d depending on the result in the BSA. From this, we obtain the experimental density matrices ρ_{exp} (see figure 3), out of which we are able to calculate the states' fidelity $\mathcal{F}$, as well as their logarithmic negativity $\mathcal{N}$ [34]. The latter is, as an entanglement measure, zero for separable states and equal to one for maximally entangled states. As one can see from table 1 we get an entangled state for each of the four Bell-state projections in the CPHASE gate with fidelities of up to 0.803 relative to the corresponding expected Bell state and with an average of 0.773 for all simultaneously detected Bell states.

Quantum teleportation enables efficient communication of quantum information between remote partners and thus is a core element of future long-distance quantum networks. From that point of view entanglement swapping is particularly useful, provided one obtains a swapped state that is entangled strongly enough to exhibit non-local correlations. To check the non-classical properties of our swapped states we show that they violate a CHSH-type Bell inequality [35]. Using the CPHASE gate this can be done at the same time for all four Bell states by measuring the correlation coefficient:

$$|S_{\pm}| := |\pm\langle\hat{A}, \hat{D}\rangle \mp \langle\hat{A}, \hat{d}\rangle + \langle\hat{a}, \hat{D}\rangle + \langle\hat{a}, \hat{d}\rangle|. \quad (6)$$

Herein $\langle\hat{A}, \hat{D}\rangle$, $\langle\hat{A}, \hat{d}\rangle$, $\langle\hat{a}, \hat{D}\rangle$ and $\langle\hat{a}, \hat{d}\rangle$ are the expectation values of four local operators that correspond to a polarization measurement under four sets of angles; 0° for $\hat{a}$, -22.5° for $\hat{D}$,

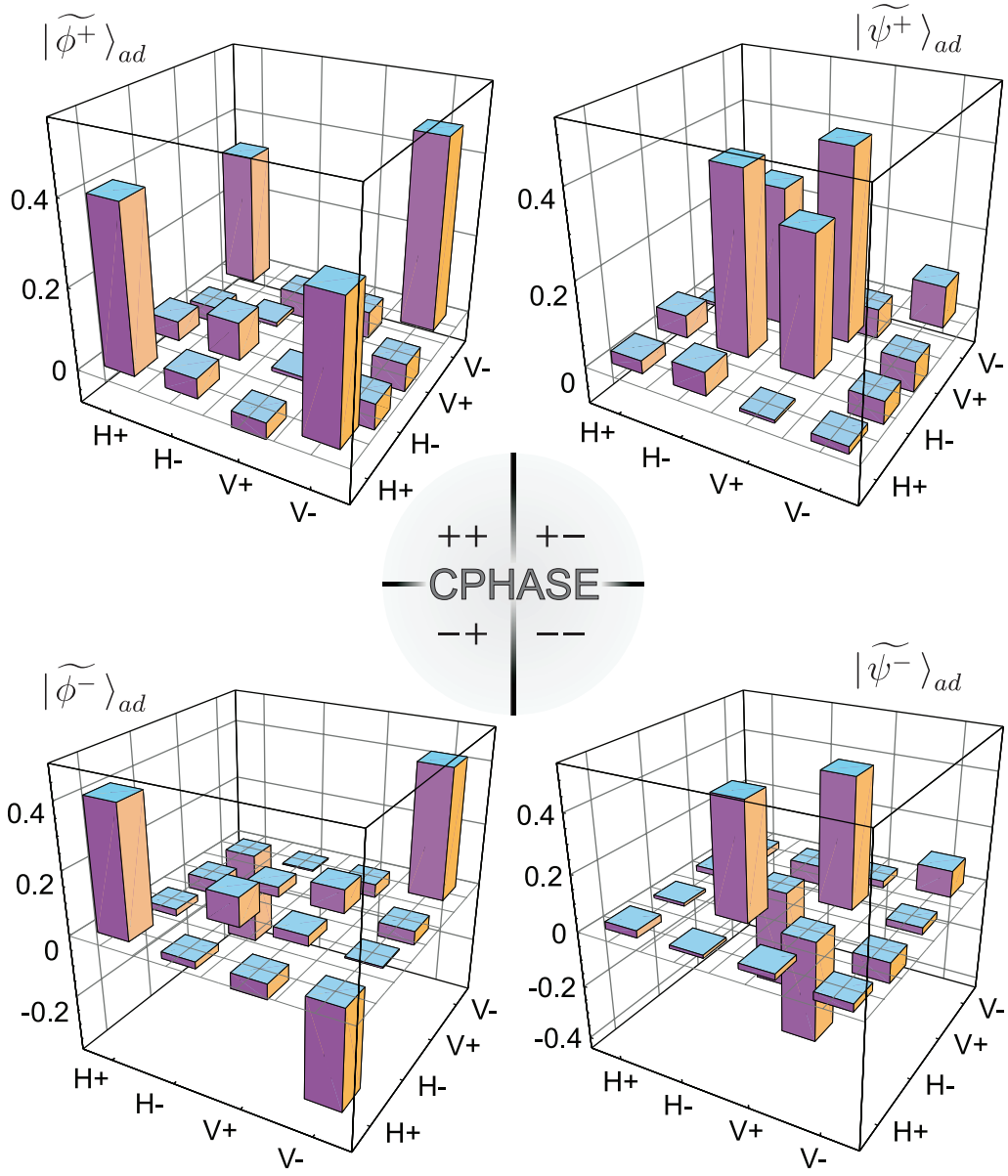

Figure 3. Experimentally reconstructed density matrix ρ_{exp} of the swapped states. Different outcomes of the projection measurement in the CPHASE gate result in different swapped states. In all four cases, the four columns, which are significantly different from noise, clearly signal the respective swapped, entangled state with high fidelity.

-45° for $\hat{A}$ and -67.5° for $\hat{d}$, respectively. $\hat{A}$, $\hat{a}$ are acting on qubits in mode a and $\hat{D}$, $\hat{d}$ on qubits in mode d.

For local hidden variable models $|S_\pm|$ is bounded from above by 2. In our experiment we were able to violate this limit for each of the four Bell states ($|\tilde{\phi}^+\rangle_{ad} : S_+ = -2.20 \pm 0.17$, $|\tilde{\psi}^+\rangle_{ad} : S_+ = 2.13 \pm 0.15$, $|\tilde{\phi}^-\rangle_{ad} : S_- = 2.12 \pm 0.16$, $|\tilde{\psi}^-\rangle_{ad} : S_- = -2.12 \pm 0.18$). Due to the limited measurement time for each of the four cases the error is relatively high compared to the

actual violation. However, the average value of 2.14 ± 0.08 confirms the violation of the Bell inequality.

3. Discussion and conclusion

To summarize, we have performed complete BSA in a teleportation and entanglement swapping experiment by applying a probabilistic, linear optics CPHASE gate for photons. The teleported polarization states showed fidelities clearly above the classical bound. The quality of the implemented teleportation and the fact that we were able to achieve an efficient quantum channel was confirmed by reconstruction of the quantum process matrix. Running the entanglement swapping protocol yields high fidelities and states that are entangled strongly enough to violate a Bell inequality. So, a universal two-photon gate based on linear optics was successfully applied for the first time in quantum communication protocols.

Our experiment is a further demonstration that linear optics gates are no longer feasible just in principle, but have reached a level of functionality and simplicity that allows their implementation in quantum information applications. The combination with recently developed active feed-forward techniques [36] will additionally open up new vistas for linear optics quantum computation.

Acknowledgments

This work was supported by the DFG-Cluster of Excellence MAP and the European Commission through the EU Project RamboQ and QAP. RU and AZ acknowledge support by QCCM.

References

[1] Bennett C H, Brassard G, Crépeau C, Jozsa R, Peres A and Wootters W K 1993 Teleporting an unknown quantum state via dual classical and Einstein–Podolsky–Rosen channels *Phys. Rev. Lett.* **70** 1895–9
[2] Żukowski M, Zeilinger A, Horne M A and Ekert A K 1993 "Event-ready-detectors" Bell experiment via entanglement swapping *Phys. Rev. Lett.* **71** 4287–90
[3] Nielsen M A, Knill E and LaFlamme R 1998 Complete quantum teleportation using nuclear magnetic resonance *Nature* **396** 52–5
[4] Furusawa A, Sørensen J, Braunstein S, Fuchs C, Kimble J and Polzik E 1998 Unconditional quantum teleportation *Science* **282** 706–9
[5] Riebe M *et al* 2004 Deterministic quantum teleportation with atoms *Nature* **429** 734–7
[6] Barrett M D *et al* 2004 Deterministic quantum teleportation of atomic qubits *Nature* **429** 737–9
[7] Kim Y-H, Kulik S P and Shih Y 2001 Quantum teleportation of a polarization state with a complete Bell state measurement *Phys. Rev. Lett.* **86** 1370–3
[8] Schuck C, Huber G, Kurtsiefer C and Weinfurter H 2006 Complete deterministic linear optics Bell state analysis *Phys. Rev. Lett.* **96** 190501
[9] Bouwmeester D, Pan J W, Mattle K, Eibl M, Weinfurter H and Zeilinger A 1997 Experimental quantum teleportation *Nature* **390** 575–9
[10] Pan J W, Bouwmeester D, Weinfurter H and Zeilinger A 1998 Experimental entanglement swapping: entangling photons that never interacted *Phys. Rev. Lett.* **80** 3891–4
[11] Weinfurter H 1994 Experimental Bell-state analysis *Europhys. Lett.* **25** 559

[12] Braunstein S L and Mann A 1995 Measurement of the Bell operator and quantum teleportation *Phys. Rev.* A **51** R1727–30
[13] van Houwelingen J A W, Brunner N, Beverators A, Zbinden H and Gisin N 2006 Quantum teleportation with a three-Bell-state analyzer *Phys. Rev. Lett.* **96** 130502
[14] Knill E, Laflamme R and Milburn G J 2001 A scheme for efficient quantum computation with linear optics *Nature* **409** 46–52
[15] Ralph T C, Langford N K, Bell T B and White A G 2002 Linear optical controlled-NOT gate in the coincidence basis *Phys. Rev.* A **65** 062324
[16] Hofmann H F and Takeuchi S 2002 Quantum phase gate for photonic qubits using only beam splitters and postselection *Phys. Rev.* A **66** 024308
[17] Gasparoni S, Pan J W, Walther P, Rudolph T and Zeilinger A 2004 Realization of a photonic controlled-NOT gate sufficient for quantum computation *Phys. Rev. Lett.* **93** 020504
[18] Pittman T B, Jacobs B C and Franson J D 2002 Demonstration of nondeterministic quantum logic operations using linear optical elements *Phys. Rev. Lett.* **88** 257902
[19] Sanaka K, Jennewein T, Pan J-W, Resch K and Zeilinger A 2004 Experimental nonlinear sign-shift for linear optics quantum computation *Phys. Rev. Lett.* **92** 017902
[20] O'Brien J L, Pryde G J, White A G, Ralph T C and Branning D 2003 Demonstration of an all-optical quantum controlled-NOT gate *Nature* **426** 264–7
[21] Langford N K, Weinhold T J, Prevedel R, Gilchrist A, O'Brien J L, Pryde G J and White A G 2005 Demonstration of a simple entangling optical gate and its use in Bell-state analysis *Phys. Rev. Lett.* **95** 210504
[22] Kiesel N, Schmid C, Weber U, Ursin R and Weinfurter H 2005 Linear optics controlled-phase gate made simple *Phys. Rev. Lett.* **95** 210505
[23] Okamoto R, Hofmann H F, Takeuchi S and Sasaki K 2005 Demonstration of an optical quantum controlled-NOT gate without path interference *Phys. Rev. Lett.* **95** 210506
[24] Politi A, Cryan M J, Rarity J G, Yu S and O'Brien J L 2008 Silica-on-silicon waveguide quantum circuits *Science* **320** 646–9
[25] Clark A S, Fulconis J, Rarity J G, Wadsworth W J and O'Brien J L 2008 An all optical fibre quantum controlled-NOT gate arXiv:0802.1676v1 [quant-ph]
[26] Lütkenhaus N, Calsamiglia J and Suominen K-A 1999 Bell measurements for teleportation *Phys. Rev.* A **59** 3295–300
[27] Vaidman L and Yoran N 1999 Methods for reliable teleportation *Phys. Rev.* A **59** 116–25
[28] Eisert J, Wilkens M and Lewenstein M 1999 Quantum games and quantum strategies *Phys. Rev. Lett.* **83** 3077
[29] Schmid C, Kiesel N, Wieczorek W, Weinfurter H, Mintert F and Buchleitner A 2008 Experimental direct observation of mixed state entanglement *Phys. Rev. Lett.* A **101** 260505
[30] James D, Kwiat P, Munro W and White A 2001 Measurement of qubits *Phys. Rev.* A **64** 052312
[31] Chuang I L and Nielsen M A 1997 Prescription for experimental determination of the dynamics of a quantum black box *J. Mod. Opt.* **44** 2455–67
[32] O'Brien J L, Pryde G J, Gilchrist A, James D F V, Langford N K, Ralph T C and White A G 2004 Quantum process tomography of a controlled-NOT gate *Phys. Rev. Lett.* **93** 080502
[33] Gilchrist A, Langford N K and Nielsen M A 2004 Distance measures to compare real and ideal quantum processes arXiv:quant-ph/0408063
[34] Vidal G and Werner R F 2002 Computable measure of entanglement *Phys. Rev.* A **65** 032314
[35] Clauser J F, Horne M A, Shimony A and Holt R A 1969 Proposed experiment to test local hidden-variable theories *Phys. Rev. Lett.* **23** 880–4
[36] Prevedel R, Walther P, Tiefenbacher F, Böhi P, Kaltenbaek R, Jennewein T and Zeilinger A 2006 High-speed linear optics quantum computing using active feed-forward *Nature* **445** 65–9